COMMUNICATION

Check for updates

Synthesis and properties of novel type I photosensitizer polycyclic amide†

Kui Wang, [ID] [a] Tao Ye,[a] Haoyang Du,[a] Xiangyu Jin,[a] Xiaofen Yi,[a] Huiying Gao,[a] Yuan Zhang,[a] Wei Dong,[a] Shihui Liu, [ID] [b] Jing Guan,*[a] Feng Lin*[a] and Debin Xia [ID] [bc]

Herein, we have designed and synthesized a novel type-I photosensitizer (PhPA) via Rh-catalyzed oxidative cyclization of diacetoxyterephthalamide with alkynes. The photoelectric properties, photosensitivity and photodegradation process of PhPA have been systematically investigated. The remarkable fluorescence quenching effect ($\Phi_{PL} < 0.01$) of PhPA suggests that the intersystem crossing from the singlet excited state to the reactive triplet state is enhanced by the enlarged conjugated backbone. Additionally, the ability of superoxide radical ($O_2^{-\cdot}$) generation was confirmed by electron paramagnetic resonance spectroscopy. Finally, the mechanism of PhPA photo-oxidative degradation via the structure of two metabolites is proposed.

Photodynamic therapy (PDT), emerging as a minimally invasive, highly efficient and noninvasive option for cancer treatment, has proven to be one of the most promising ways for cancer treatment in recent years.[1] In PDT treatment, reactive oxygen species (ROS) including singlet oxygen ($^1O_2$), superoxide radical ($O_2^{-\cdot}$), hydroxyl radical ($^\cdot OH$), and hydrogen peroxide (H_2O_2), are generated by photosensitizers (PSs) with irradiation.[2] There are mainly two types of PSs, based on ROS generation mechanisms. The majority of PSs (called type-II PSs) generate $^1O_2$ by directly transferring energy to molecules, and have high oxygen dependence and involve high oxygen consumption. But the tumor microenvironment (TME) is always hypoxic, which results from rapid proliferation and high oxygen consumption of tumor cells.[3] In type-I PSs, oxygen can be reacted to generate ROS ($O_2^{-\cdot}$, $^\cdot OH$) efficiently via electron transfer mechanisms

and be supplemented through the subsequent reaction process, thus being suited to the tumor hypoxic environment.[2,4]

Ideal type-I PSs should exhibit biological window absorption, good amphilicity, satisfactory biosafety and high ROS photogeneration.[2c] To date, a number of type-I macromolecule PSs have been reported, but there are still some shortcomings, like worrisome biosafety, need for high dosage, poor reproducibility, and complex pharmacokinetics.[5] Unlike macromolecules with complex components, organic molecules stand out as a promising option for practical bioapplications with their distinct advantages of favorable biocompatibility, satisfactory metabolism, facile processability, excellent reproducibility and structural diversity.[6] Therefore, it is crucial to exploit novel and superior type-I organic PSs with good biosafety, structural diversity and flexible preparation characteristics. Recently, a few type-I organic PSs, which include the sulfur substitution of carbonyl compounds,[7] compounds with a "D–π–A" (electron donor–π–electron acceptor) structure,[8] and compounds with aggregation-induced emission characteristics,[6,9] have been reported. On analyzing these varied structures, we find there are no general rules regarding how to design a specific type-I PS.

Besides, many PSs or potential PSs including indocyanine green, methylene blue, and Rose Bengal (RB) with excellent photophysical properties are limited in application due to their poor stability.[5b,10] There is no doubt that exploring the degradation mechanisms of PSs during use is one of the important ways for us to design new PSs. However, the corresponding literature revealing the degradation mechanisms is scarce.

Herein, we report a potential heavy-atom-free organic type-I PS, named PhPA, with easy modifiable structure, facile synthesis and high ROS generation ability under white light irradiation. Furthermore, density functional theory (DFT) was employed to support the experimental results. Additionally, the ability to generate ROS was investigated. In order to solve the water solubility problem of PhPA, the FDA-approved Pluronic F127 was used to encapsulate PhPA, yielding nanoparticles (PhPA@F127NPs). We further explored the structure of its

[a]Department of Organic Chemistry, College of Pharmacy, Harbin Medical University, Harbin, China. E-mail: guanjing@ems.hrbmu.edu.cn; xiaolin_linfeng@126.com

[b]MIIT Key Laboratory of Critical Materials Technology for New Energy Conversion and Storage, School of Chemistry and Chemical Engineering, Harbin Institute of Technology, Harbin, China

[c]State Key Laboratory of Urban Water Resource and Environment, Harbin Institute of Technology, Harbin, China

metabolites with single-crystal X-ray diffraction to gain more insight into the photodegradation mechanism of PhPA.

The synthesis route and the structures of target compounds PA and PhPA are shown in Scheme 1. Intermediate PA was facilely obtained in a yield of 75% by Rh-catalyzed cyclization coupling using N^1,N^4-diacetoxyterephthalamide (DAPA) and 1,2-bis(4-(tert-butyl)phenyl)ethyne as starting materials. The target compound PhPA was produced by Rh-catalyzed oxidative cyclization using PA and relevant alkyne with a yield of 58%. The structures of all obtained compounds were confirmed by nuclear magnetic resonance spectroscopy and mass spectrometry, and their corresponding spectra are also shown in Fig. S2–S8† in the ESI.† Moreover, the structure of PhPA was characterized by single crystal X-ray diffraction.

To examine the optical properties of compounds PA and PhPA, UV-visible absorption and fluorescence spectroscopies were employed. The UV-visible absorption spectra show that PA has a broad absorption from 300 to 500 nm, while the broad absorption peaks of PhPA are redshifted almost 100 nm (400 to 600 nm) through the enlarged molecular backbone, qualifying their potential as an ideal PS for white-light harvesting. The enlarged molecular backbone in PhPA is expected to redshift the absorption spectra to the near biological window through effective HOMO destabilization and LUMO stabilization (Fig. 1a). Additionally, the emission spectrum shows that the emission maximum of PA is at 481 nm. The maximum emission peak of PhPA is at 583 nm (Fig. 1b). It also shows that the conjugated length increasing from compound PA to PhPA has a substantial effect upon their photophysical properties. PA exhibits intense fluorescence with good quantum yields ($\Phi_{PL} = 0.16$). In sharp contrast, PhPA exhibits low luminescence efficiencies ($\Phi_{PL} < 0.01$). The fluorescence quenching suggests that the intersystem crossing (ISC) process from the singlet excited state to the triplet excited state was enhanced.

To gain more insight into the electronic properties and the mechanism of triplet state formation of these compounds, frontier molecular orbitals were calculated with the Gaussian 09 program using DFT and time-dependent DFT calculations at the B3LYP/6-31G** level. As depicted graphically in Fig. 2a, the
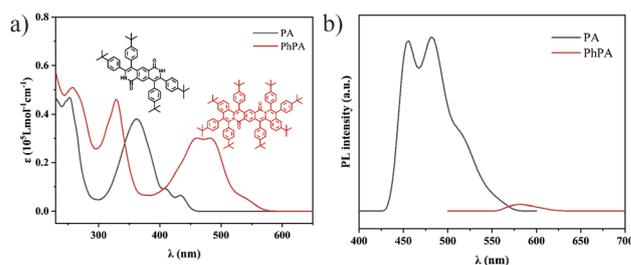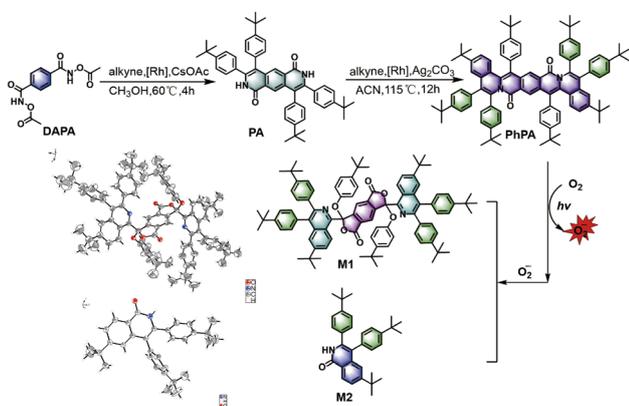

Fig. 1 (a) Absorption spectra of PA and PhPA in DCM (concentration: 10 μM). (b) PL spectra of PA and PhPA in DCM (concentration: 10 μM; λ_{ex} = 360 and 483 nm, respectively).

target products have well delocalized electron distributions in their LUMOs and HOMOs. The simulation results reveal that the HOMO–LUMO electron distribution presented a centrosymmetric arrangement, the LUMO orbitals possessed delocalized electron distribution covering the conjugated skeleton, and are not limited to the electron-withdrawing part. Moreover, the enlarged molecular backbone has an obvious effect on electron distributions, the HOMO electron distribution being delocalized with molecular backbone enlarging, while it is not observed in LUMOs. It is universally acknowledged that k_{ISC} is negatively correlated with the singlet–triplet energy gap (ΔE_{ST}). Indeed, ΔE_{ST} decreases with an enlarged molecular backbone, resulting in a tremendous enhancement in the ISC rate constant (k_{ISC}), for PhPA, and the ISC from the S_2 state to the T_4 state may be the dominant contributor to the formation of the triplet state (ESI, Fig. S22†). To gain an in-depth understanding of the electronic behavior of PhPA, cyclic voltammetry (CV) and differential pulse voltammetry (DPV) experiments were conducted at room temperature, using 0.1 M tetrabutylammonium perchlorate as the supporting electrolyte, and the CV curves are shown in Fig. 2b. Two reversible redox peaks are observed in the CV curves. The first oxidation potentials were 0.77 and 0.32 V (relative to ferrocene), respectively. With the conjugation length increasing from PA to PhPA, the first oxidation wave potential decreased. Based on the first oxidation wave, the HOMO energy levels were calculated to be −5.47 and −5.02 eV, respectively. These results agree well with the trends derived from the DFT calculations.

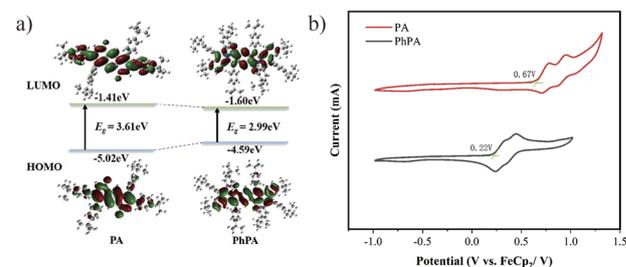Scheme 1 Synthetic route to and degradation of PhPA, and the single crystal structures of two metabolites (M1 and M2).

Fig. 2 (a) Frontier molecular orbital diagram of the target products in their ground state (S_0). (b) CV curves of target products in CH_2Cl_2 and 0.1 M Bu_4NPF_6 on a Pt electrode at a scan rate of 50 mV s^{-1} vs. Ag/AgCl wire.

Inspired by the remarkable fluorescence quenching upon conversion of PA and PhPA, we then evaluated their ROS generation efficiency to elucidate the triplet state formation. As is known, the 1,3-diphenylisobenzofuran (DPBF) probe can be easily oxidized by reactive oxygen radical, which results in the absorption intensity decreasing at 410 nm.[11] The ROS generation of PSs was further assessed in DCM using DPBF as a ROS probe with white light irradiation. Meanwhile, RB, a commercial PS, was employed as a reference. As illustrated in Fig. 3a, we found that the absorption of DPBF treated with PhPA and RB at 410 nm shows obvious attenuation with irradiation time. PhPA exhibits moderate ROS yield, and the ROS signal was not detected for PA under identical conditions. Then, we evaluated the $^1O_2$ generation capability of PhPA by using 9,10-anthracenediylbis (methylene)dimalonic acid (ABDA) as a $^1O_2$ indicator, under white light irradiation.[12] In the presence of singlet oxygen, ABDA will be irreversibly oxidized, and its characteristic absorption peak will be significantly reduced. The yield of singlet oxygen will be specifically evaluated by the change of absorption of ABDA at 400 nm. As shown in Fig. 3b, unexpectedly, the $^1O_2$ signal was not detected for PhPA. Meanwhile, characteristic absorption peaks (340 and 483 nm) of PhPA continuously decreased under white light irradiation. Based on the previous results, we speculate that PhPA might be a new type-I PS. Electron paramagnetic resonance (EPR) experiments were carried out to examine the active species of oxygen. 5,5-Dimethyl-1-pyrroline-N-oxide (DMPO) was employed to trap the active species of $O_2^{-\bullet}$.[13] As expected, no EPR signal was observed

in PhPA solution in the dark, but a characteristic paramagnetic DMPO–OOH signal attributed to the addition of DMPO and $O_2^{-\bullet}$ emerged under irradiation with a xenon lamp with a 400–700 nm light filter for 3 minutes (ESI, Fig. S13†). Furthermore, we encapsulated PhPA into NPs using Pluronic F127 as the encapsulation matrix. The obtained PhPA@F127 NPs were characterized by dynamic light scattering. The average hydrodynamic size (D_h) was measured to be 114.8 nm (Fig. S17†). Then, we detected the formation of $O_2^{-\bullet}$ in water with DHE. These results show that the addition of compound PhPA can distinctly increase the fluorescence intensity of DHE with irradiation during 20 s (Fig. 3d). Considering these results, we can reasonably speculate that PhPA predominately underwent electron transfer in a PDT process. In addition, as shown in Fig. 3b and c, continuous decomposition of PhPA was observed with sustained irradiation. This is the reason why the increasing fluorescence intensity rate of DHE becomes slower.

Considering the degradation of PhPA, the photostabilities of PA and PhPA were investigated by UV–visible absorption and fluorescence spectroscopy in dichloromethane. In this process, we found the photostability of PA to be average, while PhPA is very sensitive to irradiation. According to the results and previous considerations, the reason why PhPA is unstable is that PhPA can be easily oxidized by $O_2^{-\bullet}$. High ROS generation efficiency induces a high degradation rate of PhPA. These results agree well with the trends derived from photosensitivity experiments.
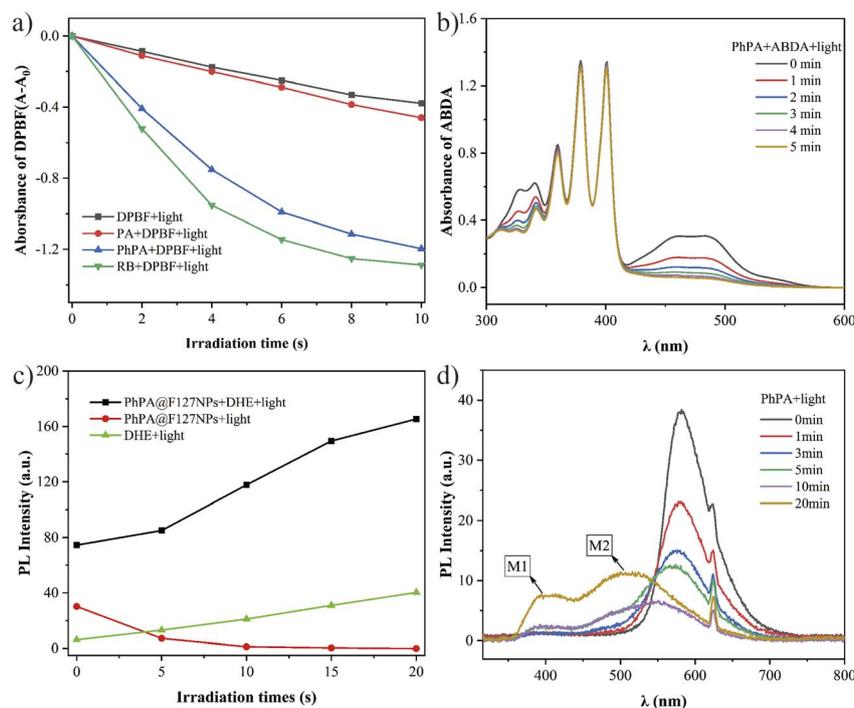

Fig. 3 (a) Comparison of ROS generation of PA, PhPA and Rose Bengal at equal concentration (10 μM). (b) Time-dependent decrease of absorbance of ABDA in the presence of PhPA in DCM (10 μM). (c) Comparison of $O_2^{-\bullet}$ probe's fluorescence intensity at 590 nm after irradiation for different times detected by using dihydroethidium (DHE) as a probe (50 μM; λ_{ex} = 510 nm, λ_{em} = 590 nm). (d) PL spectra of PhPA (25 μM; λ_{ex} = 312 nm) in DCM irradiated by white light for 0, 1, 3, 5, 10, and 20 min. All irradiation was by a white light (5 mW cm^{-2}).

To confirm the structure of metabolites and further elucidate the mechanism of oxidative metabolic processes, we purified the metabolites by a silica gel column to afford two compounds which are M1 and M2. Compounds M1 and M2 were investigated by UV-visible absorption and fluorescence spectroscopies in dichloromethane. On comparing the fluorescence emission spectra of metabolites M1 (390 nm) and M2 (510 nm), we found that the two emission peaks of metabolites correspond to M1 and M2, respectively (Fig. 3d). The structures of M1 and M2 were characterized by NMR and single crystal X-ray diffraction.

Lastly, the mechanism of photo-oxidative degradation via superoxide radical produced by PhPA with irradiation is proposed (Scheme 2). The oxidation mechanism of PhPA involves the following steps. (1) Under irradiation, the ground-state PhPA can convert to the excited singlet state, then can de-excite into the long-lived triplet state through ISC. Triplet state PS can form cation and anion radicals (PhPA$^{+\cdot}$ and PhPA$^{-\cdot}$), which can subsequently react with molecular oxygen to generate $O_2^{-\cdot}$.[2b,c,14] (2) PhPA$^{+\cdot}$ was oxidized by $O_2^{-\cdot}$ which gave 1,2-dioxetane 1 by [2 + 2] cycloaddition. The metabolite M1 was formed by facile homolytic cleavage of the O–O bond, radical 1,2-aryl migration and the process of typical addition–elimination. The starting molecule PhPA$^{+\cdot}$ breaks into three fragments due to another fragmentation pathway of 1,2-dioxetane 1. The mechanism is suggested in that a double β-cleavage produces two carbonyls that leads to the formation of compound 5 (ESI, Fig. S33†). The metabolite M2 is formed after hydrolysis by compound 5.

In summary, we demonstrated a completely new, heavy-atom-free and type-I PS with excellent potential, and confirmed its great ability for ROS generation. Our findings revealed that PhPA has very broad absorption from 400 to 600 nm, qualifying it as an ideal PS for white-light harvesting. According to the theoretical calculations, ΔE_{ST} decreases upon enlarged molecular backbone. We analyzed and confirmed the structures of metabolites M1 and M2 by NMR and single crystal

X-ray diffraction, then we supposed a mechanism of photo-oxidative degradation via superoxide radical produced by PhPA with irradiation. On changing tert-butyl in eight aromatic rings to other substituents with special functional groups, this structure may take on some distinctive desired function. The development of other derivatives based on this structure to solve the problem of poor photostability is in progress.

Author contributions

X. Y. J., X. F. Y. and H. Y. G. explored the experimental route in the early stage. K. W., T. Y. and H. Y. D. performed the experiments and analyses. K. W. wrote the paper. Y. Z., W. D. and S. H. L. conducted the photophysical and electrochemical experiments. D. B. X. revised the paper. G. J., F. L. and K. W. conceived the idea and supervised the research.
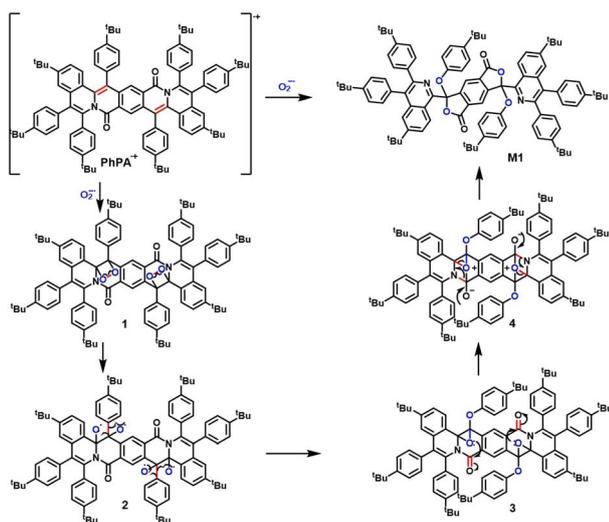
Conflicts of interest

There are no conflicts to declare.

Acknowledgements

Notes and references

1 D. E. Dolmans, D. Fukumura and R. K. Jain, Nat. Rev. Cancer, 2003, 3, 380–387.

2 (a) B. Yang, Y. Chen and J. Shi, Chem. Rev., 2019, 24, 4881–4985; (b) Y.-Y. Wang, Y.-C. Liu, H. Sun, et al., Coord. Chem. Rev., 2019, 395, 46–62; (c) D. Chen, Q. Xu, W. Wang, et al., Small, 2021, 17.

3 Z. Yin, D. Chen, J. Zou, J., et al., ChemistrySelect, 2018, 3, 4366–4373.

4 (a) Q. Sun, Q. Su, Y. Gao, et al., Aggregate, 2022, e298; (b) K. Chen, P. He, Z. Wang and B. Z. Tang, ACS Nano, 2021, 15, 7735–7743; (c) Z. Zhou, J. Song, L. Nie and X. Chen, Chem. Soc. Rev., 2016, 45, 6597–6626.

5 (a) G. Lan, K. Ni, S. S. Veroneau, et al., J. Am. Chem. Soc., 2019, 141, 4204–4208; (b) G. Xu, C. Li, C. Chi, et al., Nat. Commun., 2022, 13, 3064; (c) K. Chen, R. Xing and X. Yan, Aggregate, 2021, 2, 84–94; (d) R. C. Gilson, K. C. L. Black, D. D. Lane, et al., Angew. Chem., Int. Ed. Engl., 2017, 56, 10717–10720; (e) Z. Lv, H. Wei, Q. Li, et al., Chem. Sci., 2018, 9, 502–512; (f) X. Y. Wu, M. S. Xu, S. N. Wang, et al., Dalton Trans., 2022, 51, 2296–2303; (g) J. L. Tong, X. Y. Yang, X. X. Song, et al., Dalton Trans., 2023, 52, 1105–1112.

6 D. Li, P. Liu, Y. Tan, Z. Zhang, M. Kang, D. Wang and B. Z. Tang, Biosensors, 2022, 12, 722.

Scheme 2 Mechanism of PhPA photo-oxidative degradation.

7 V. N. Nguyen, S. Qi, S. Kim, et al., J. Am. Chem. Soc., 2019, 141, 16243–16248.

8 (a) S. Zhou, R. Li, Y. Li, et al., J. Mater. Chem. B, 2022, 10, 8003–8012; (b) J. Qu, Y. Zhang, Z. Cai, et al., Nanoscale, 2022, 14, 14064–14072; (c) Y. Wang, J. Li, Y. Zhang, et al., Chem. Commun., 2022, 58, 7797–7800; (d) Z. Zhuang, J. Dai, M. Yu, et al., Chem. Sci., 2020, 11, 3405–3417; (e) W. Chen, Y. Zhang, H. B. Yi, et al., Angew. Chem., Int. Ed. Engl., 2023, 62, e202300162; (f) S. Liu, B. Wang, Y. Yu, et al., ACS Nano, 2022, 16, 9130–9141; (g) J. Gong, L. Liu, C. Li, et al., Chem. Sci., 2023, 14, 4863–4871.

9 (a) Z. Liu, Q. Wang, W. Qiu, et al., Chem. Sci., 2022, 13, 3599–3608; (b) M. M. S. Lee, D. M. Lin, J. H. C. Chau, et al., ACS Nano, 2023, 17(11), 11039–11053.

10 J. Qi, Y. Fang, R. T. K. Kwok, et al., ACS Nano, 2017, 11, 7177–7188.

11 P. Carloni, E. Damiani, L. Greci, et al., Res. Chem. Intermed., 1993, 19, 395–405.

12 N. A. Kuznetsova, N. S. Gretsova, O. A. Yuzhakova, et al., Russ. J. Gen. Chem., 2001, 71, 36–41.

13 J. Liu, K. Zhang, Z. Chen, et al., Chem. – Asian J., 2020, 15, 1118–1124.

14 (a) J. Davila and A. Harriman, Photochem. Photobiol., 1989, 50, 29–35; (b) J. Li, Z. Zhuang, Z. Zhao and B. Z. Tang, VIEW, 2021, 3, 20200121.